Chemical Research in Toxicology

Article

pubs.acs.org/crt

Bioactivation of Nevirapine to a Reactive Quinone Methide: Implications for Liver Injury

Amy M. Sharma,[†] Yan Li,[‡] Maria Novalen,[†] M. Anthony Hayes,[§] and Jack Uetrecht*,[†]

[†]Leslie Dan Faculty of Pharmacy, University of Toronto, Toronto, Ontario, Canada M5S 3M2

[‡]Therapure Biopharma Inc., 2585 Meadowpine Boulevard, Mississauga, Ontario, L5N 8H9

[§]Department of Pathobiology, Ontario Veterinary College, University of Guelph, Ontario N1G 2W1, Canada

ABSTRACT: Nevirapine (NVP) treatment is associated with a significant incidence of liver injury. We developed an anti-NVP antiserum to determine the presence and pattern of covalent binding of NVP to mouse, rat, and human hepatic tissues. Covalent binding to hepatic microsomes from male C57BL/6 mice and male Brown Norway rats was detected on Western blots; the major protein had a mass of ~55 kDa. Incubation of NVP with rat CYP3A1 and 2C11 or human CYP3A4 also led to covalent binding. Treatment of female Brown Norway rats or C57BL/6 mice with NVP led to extensive covalent binding to a wide range of proteins. Co-treatment with 1-aminobenzotriazole dramatically changed the pattern of binding. The covalent binding of 12-hydroxy-NVP, the pathway that leads to a skin rash, was much less than that of NVP, both *in vitro* and *in vivo*. An analogue of NVP in which the methyl hydrogens were replaced by deuterium also produced less covalent binding than NVP. These data provide strong evidence that covalent binding of NVP in the liver is due to a quinone methide formed by oxidation of the methyl group. Attempts were made to develop an animal model of NVP-induced liver injury in mice. There was a small increase in ALT in some NVP-treated male C57BL/6 mice at 3 weeks that resolved despite continued treatment. Male Cbl-b$^{-/-}$ mice dosed with NVP had an increase in ALT of >200 U/L, which also resolved despite continued treatment. Liver histology in these animals showed focal areas of complete necrosis, while most of the liver appeared normal. This is a different pattern from the histology of NVP-induced liver injury in humans. This is the first study to report hepatic covalent binding of NVP and also liver injury in mice. It is likely that the quinone methide metabolite is responsible for NVP-induced liver injury.

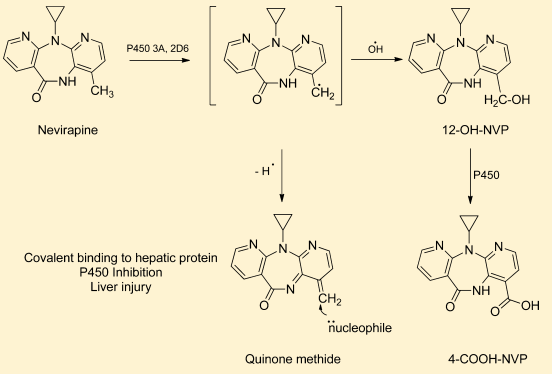

INTRODUCTION

Nevirapine (NVP, Viramune, TOC graphic) is a non-nucleoside reverse transcriptase inhibitor used for the treatment of HIV-1 infections. Treatment with NVP is associated with a significant incidence of idiosyncratic skin rashes and/or liver toxicity.[1] The incidence of skin rashes is approximately 9%. They are usually mild to moderate in nature; however, 16% of NVP-induced rashes are very severe, including Stevens-Johnson syndrome and toxic epidermal necrolysis.[2] In 2000, the FDA placed a black box warning on NVP due to hepatotoxicity, which occurs in 6% of patients and can be life threatening.[2] The incidence of elevated serum alanine transaminase (ALT) in NVP-treated patients, which is the first indication of liver injury, is between 8 and 18% and typically occurs within the first six weeks of treatment.[3] Liver injury normally resolves when the drug is stopped, but it can lead to fulminant liver failure and death. There also exists evidence for increased risk of liver injury in non-HIV patients, which may be due to higher CD4 cell counts.[4]

The mechanisms of idiosyncratic liver injury and skin rashes are currently unknown, but most idiosyncratic drug reactions appear to be mediated by reactive metabolites. We developed an animal model of NVP-induced skin rash in Brown Norway (BN) rats that is clearly immune-mediated and has characteristics very similar to the rash in humans; however, the rats did not develop liver toxicity.[1,5] We postulated that the 12-hydroxylation pathway was involved in the induction of the skin rash; therefore, we replaced the hydrogens on the methyl group with deuterium to slow down the rate of 12-hydroxylation (TOC graphic). We found that this analogue (DNVP) did not cause a skin rash as predicted, but instead of higher blood levels because one of the major metabolic pathways was inhibited, we found that the blood levels of DNVP were actually much lower than those of NVP at the same dose.[6] Although the reason for this was not immediately obvious, we ultimately concluded that, in addition to oxygen rebound to form 12-OH-NVP, the intermediate free radical in the P450-mediated oxidation could also lose a hydrogen atom to form a reactive quinone methide (TOC graphic). A glutathione conjugate consistent with the quinone methide intermediate has been reported;[7,8] however, it could also come from a sulfate conjugate of the 12-OH-NVP.

In this study, we used an antiserum against NVP to study the covalent binding of NVP, DNVP, and 12-OH-NVP to hepatic

Received: April 18, 2012
Published: July 13, 2012

dx.doi.org/10.1021/tx300172s | *Chem. Res. Toxicol.* 2012, 25, 1708–1719

Scheme 1. Synthetic Pathway of the Immunogen Used for the Induction of Anti-NVP Antiserum

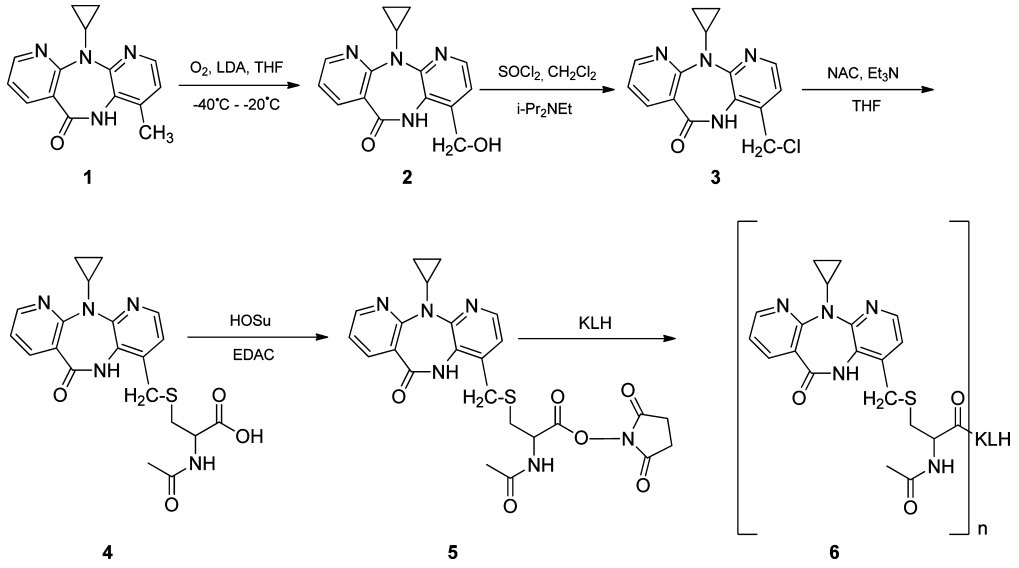

proteins in mice, rats, and humans. We also studied the effects of chronic administration of NVP to various strains of mice to determine if it causes liver injury. In addition to C57BL/6 and BALB/c, we included the Casitas B-lineage lymphoma-B (Cbl-b) knockout mouse (Cbl-b$^{-/-}$), which is bred on a C57BL/6 background. The Cbl gene is a mammalian gene that encodes a variety of proteins, specifically those involved in cell signaling and protein ubiquitination. Lack of ubiquitination of NVP protein adducts could lead to more persistent covalent binding and possibly toxicity. This also impairs immune tolerance; therefore, if the liver injury is immune-mediated, these animals should be at increased risk. These animals also express a mouse isoform of CYP3A4 (CYP3A11); therefore, oxidative metabolism of NVP should occur,[9] and this has the potential to lead to liver injury.

MATERIALS AND METHODS

Chemical Materials. NVP was kindly supplied by Boehringer-Ingelheim Pharmaceuticals Inc. (Ridgefield, CT). The majority of chemical reagents (1-aminobenzotriazole (ABT), tris(hydroxymethyl)-aminomethane base, methanol, DMSO, phosphate-buffered saline (PBS, pH 7.4), glycerol, silica gel, etc.) were obtained from Sigma-Aldrich (Oakville, ON) unless otherwise noted in the methods. Ammonium persulfate was obtained from Fisher Scientific (Fair Lawn, NJ). Sodium dodecyl sulfate and Tween-20 were obtained from BioShop (Burlington, ON). Stock acrylamide/bis solution (29:1, 3.3% C), nonfat blotting grade milk powder, and nitrocellulose membrane (0.2 μM) were purchased from Bio-Rad (Hercules, CA). Ultra pure tetramethylethylenediamine was purchased from Invitrogen (Carlsbad, CA). Amersham ECL Plus Western Blotting Detection System was obtained from GE Healthcare (Oakville, ON). Horseradish peroxidise-conjugated goat antirabbit IgG (H + L chains) and monoclonal GAPDH were purchased from Sigma-Aldrich (St. Louis, Mo). Normal goat serum was obtained from Invitrogen (Grand Island, NY). Expressed human CYP3A4, rat CYP3A1, and rat CYP2C11 (each with P450 reductase and cytochome b_5), 0.5 M potassium phosphate at pH 7.4, and NADPH regenerating system solutions A and B were purchased from BD Biosciences (Woburn, MA).

Instruments and Software. AlphaEaseFC (FluorChem 8800), manufactured by Alpha Innotech, now Cell Biosciences Santa Clara, California, USA, was used to image blots. Integrated density values were obtained using the SPOT DENSO function on the FluorChem 8800 Imager.

Synthesis of 12-Trideutero-NVP (DNVP). Synthesis of DNVP was carried out using the method described by Chen et al.[6] ^{1}H NMR ($CDCl_3$): δ 0.31−0.41 (m, 2H), 0.83−0.90 (m, 2H), 3.60−3.64 (m, 1H), 7.06 (d, J = 4.8 Hz, 1H), 7.19 (dd, J = 4.8, 7.5 Hz, 1H), 8.01 (dd, J = 2.1, 6.6 Hz, 1H), 8.08 (d, J = 4.8 Hz, 1H), 8.50 (dd, J = 1.8, 4.8 Hz, 1H), 9.90 (bs, 1H). ESI-MS: m/z (%) 270 (MH^+, 100%). The ratio of the peaks at m/z 267:268:269:270 as determined by mass spectrometry was 0:0.007:0.124:0.869, indicating only trace amounts of NVP.

Production of Anti-NVP Anti-Serum in Male White New Zealand Rabbits. *Synthesis of NVP-NAC Conjugate.* The synthesis of the immunogen is outlined in Scheme 1. The first step in producing the anti-NVP antiserum was to synthesize 12-OH-NVP (**2**) and convert this to the benzylic chloride (12-Cl-NVP, **3**). The method to produce 12-OH-NVP followed the protocol described previously[10] with minor modifications. ESI-MS; m/z (%) 283 (MH+, 100%). To convert 12-OH-NVP to 12-Cl-NVP, we followed the method of Kelly et al.[11] To 12-OH-NVP (200 mg) in dry dichloromethane (10 mL) at 0 °C was added *N*,*N*-diisopropylethylamine (0.14 mL) followed by thionyl chloride (3 mL), and it was stirred under argon at room temperature for 3 h after which the thionyl chloride was evaporated by rotary evaporation. The reaction mixture was then extracted with ethyl acetate (3 × 10 mL). The ethyl acetate layer was washed with water (10 mL), dried over anhydrous sodium sulfate, and concentrated to yield crude product, which was purified with open column chromatography (silica gel, pore size 60 Å, 70−230 mesh, column dimensions 30 × 200 mm) eluted with 50% ethyl acetate/hexanes to yield 0.386 g of yellow solid. ESI-MS; m/z (%) 301 (MH^+, 100%).

The 12-Cl-NVP (1.78 g, 3.55 mmol) was dissolved in 18 mL of tetrahydrofuran and reacted with *N*-acetylcysteine (NAC, 2.31 g, 14.18 mmol) in 5 mL of triethylamine under argon reflux for 2 h. The crude mixture was cooled to room temperature, acidified to pH 3−4 by 1 N HCl and extracted with $CHCl_3$. The organic layer was dried over anhydrous sodium sulfate. Chloroform was removed under reduced pressure. The nevirapine-NAC conjugate was obtained as a pale yellow solid (**4**). Formation of the nevirapine-NAC conjugate was confirmed by mass spectrometry ESI-MS; m/z (%) 428 (MH^+, 100%).

Preparation of NVP-KLH Conjugate. All reagents and glassware were dried in a vacuum at 50 °C. Activation of the carboxy groups on NAC of the synthesized 12-NAC-NVP occurred as follows: to 61.4 mg 12-NAC-NVP was added 108.5 mg of *N*-hydroxysuccinimide and 103.9 mg of 1-ethyl-3-(3-dimethyllaminopropyl) carbodiimide hydrochloride. Anhydrous DMF (4 mL) was introduced via syringe at 0 °C. The entire mixture was sealed with a rubber stopper and stirred at 0 °C for 2 h under N_2. Methylene chloride (8 mL) was added, followed by washing with water (3 × 8 mL), and then the organic layer was

dx.doi.org/10.1021/tx300172s | *Chem. Res. Toxicol.* 2012, 25, 1708−1719

partially evaporated *in vacuo* to yield a pale yellow solution (0.5 mL, **5**). DMF (4 mL) was added followed by Keyhole limpet hemocyanin (KLH, 8 mg), and the mixture was stirred for 1 h at 4 °C. The reaction mixture was then concentrated under a N_2 stream, and 1 mL water was added. Centrifugal filtration was performed to collect the protein solution, which was then lyophilized. A final white powder (10.4 mg) was obtained (**6**) and stored at −20 °C. The same method was used to prepare a conjugate with bovine serum albumin (BSA) MALDI MS; *m*/*z* 67,139−68,569. The hapten density of the BSA conjugate was approximately 4.5 molecules of NVP-NAC/BSA as determined by the increase in mass on mass spectrometry.

Production of Anti-NVP-NAC-KLH-Antiserum. Polyclonal anti-NVP-NAC-KLH antibodies were raised in two individual 2 kg, male, pathogen-free New Zealand White rabbits (Charles River, Quebec) housed in the animal care facility at The Division of Comparative Medicine, University of Toronto. Each animal was immunized with the NVP-NAC-KLH conjugate (1 mg antigen + 100 μL of glycerol in 1.8 mL of phosphate buffered saline emulsified with an equal volume of Freund's complete adjuvant) subcutaneously at multiple sites. Injections with 500 μg of NVP-NAC-KLH in Freund's incomplete adjuvant divided into six to eight subcutaneous sites were repeated 4, 6, 8, and 12 weeks after the initial immunization. The animals were exsanguinated while under pentobarbital anesthesia 10 days after the final immunization. The serum was heat-inactivated at 56 °C for 30 min before being stored at −80 °C.

ELISA. NVP-NAC-BSA, BSA, or KLH (100 μL, 10 μg/mL in carbonate−bicarbonate coating buffer) were coated into the wells of a flat-bottom 96-well plate (Costar, Cambridge, MA), and the plate was incubated overnight at 4 °C. The plates were washed with ELISA wash buffer (50 mM tris(hydroxymethyl)aminomethane-buffered saline, pH 8.0, and 0.05% Tween-20) three times and blocked by the addition of 100 μL of postcoat solution (50 mM Tris-buffered saline, pH 8.0, and 1% BSA) for 30 min at room temperature. Following the blocking step, the wells were washed three times, and various dilutions of the anti-NVP-NAC-KLH antiserum or preimmune serum were added to the plates, which were then incubated at room temperature for 2.5 h. The plates were subsequently washed three times with ELISA wash buffer, and horseradish peroxidase-conjugated goat antirabbit IgG (diluted 1:5000 in postcoat solution; 100 μL) was added to each well. The ELISA plates were incubated at room temperature for 2 h. Plates were then washed three times with ELISA wash buffer. Enzyme substrate (3,3′,5,5′-tetramethylbenzidine peroxidase substrate and peroxidase solution B, Kirkegaard & Perry Laboratories) was mixed in equal volumes, and 100 μL of the enzyme substrate was added to each well. The plate was incubated in the dark at room temperature for 10 min. Sulfuric acid (2M, 100 μL) was added to each well to quench the reaction. Absorbance was measured with the Basic End point Option of SoftMax Pro 5 Software, using the SPECTRA maxPLUS384 plate reader (Molecular Devices Technologies) set at 450 nm.

Animal Care. Male (200−250 g) or female BN rats (150−175 g) were obtained from Charles River (Montreal, Quebec). Rats were housed in pairs in standard cages in a 12:12 h light/dark cycle with access to water and Agribrands powdered lab chow diet (Leis Pet Distribution, Inc. Wellesley, Ontario) ad libidum. Following a one week acclimatization period, rats were either maintained on control chow or started on drug containing diet (treatment groups). The drug was mixed thoroughly with powdered lab chow if it was to be administered orally. The amount of drug administered to animals was calculated based on body weight of the rats and their daily food intake. Rats were sacrificed via CO_2 asphyxiation.

Male Balb/c or C57BL/6 mice (6−8 weeks age) were obtained from Charles River (Montreal, Quebec). Cbl-b$^{-/-}$ knockout mice were bred in house from animals first developed by Dr. J. Penninger at the Institute of Molecular Biotechnology of the Austrian Academy of Science, Vienna, with his kind permission. Mice were kept 4 per cage. The average weight gain was approximately 0.75 g per week (data not shown). NVP was administrated in lab chow following a one week acclimatization period. Animal experiments were approved by the University of Toronto Animal Care Committee in accordance with guidelines of the Canadian Council on Animal Care.

Treatment of Animals with NVP, 12-OH-NVP, DNVP, or ABT. Female BN rats were treated with NVP or DNVP at 150 mg/kg/day, or 12-OH-NVP at 159 mg/kg/day (equimolar dose) orally in standard rat chow for either 8, 10, or 21 days. Dosages were based on previous work showing the induction of rash at these levels.[5] Treatment of NVP or DNVP by s.c. injection lasted 21 days with a dose of 75 mg/kg/day of either compound. ABT was dissolved in water (20 mg/mL) and administered via gavage at a dose of 50 mg/kg/day. If ABT was to be given to animals, the dose of NVP was 50 mg/kg/day via gavage. Methylcellulose (0.5%) was used to suspend NVP or metabolites given to rats by gavage or s.c. injection. All mice were started on NVP at 950 mg/kg/day in standard chow after preliminary studies showing no apparent toxicity or mortality of mice at either 550 or 950 mg/kg/day.

Incubations with Microsomes or Supersomes. Livers were homogenized in ice-cold 1.15% KCl using a Polytron 2100 homogenizer and centrifuged at 26,400*g* for 10 min at 4 °C. The supernatant was then centrifuged at 100,000*g* for 50 min at 4 °C. The pellet was homogenized in 4 volumes of glycerol−phosphate−KCl buffer, and aliquots were stored at −80 °C. The protein concentration of the prepared microsomes was quantified using a BCA protein assay kit (Novagen, EMD Biosciences Inc.). All incubations were performed at 37 °C. NVP, 12-OH-NVP, or DNVP stock solutions were prepared in methanol, and the final methanol concentration in the reactions did not exceed 1% for any incubation.[12] The microsomal incubations consisted of 100 mM potassium phosphate buffer (pH 7.4), an NADPH-regenerating system (Solution A final concentrations, 1.3 mM NADP, 3.3 mM glucose-6-phosphate, and 3.3 mM $MgCl_2$; Solution B final concentration, 0.4 Units/mL glucose-6-phosphate-dehydrogenase) and microsomal homogenate (final protein concentration varying from 0.3 mg/mL to 15 mg/mL). EDTA·2Na (0.4 mM) was added to rat CYP3A1 and 2C11 incubations, and water was added to each incubation to reach a final volume of 400 μL for rat and mouse or 200 μL for human 3A4 incubations.[13] Incubations consisting of all reaction components except the NADPH-regenerating system or drug were preincubated for 5 min. The NADPH-regenerating system or drug was added to each of the test and control tubes after the 5 min of preincubation. Reactions were stopped by placing the sample vials on dry ice and storing at −80 °C.[13] If microsomal incubations were to be analyzed via LC/MS, 250 μL of ice cold acetonitrile was used to quench the reaction, and internal standard (ethyl-NVP − a NVP derivative in which the cyclopropyl group has been replaced with an ethyl group, 5.4 μg/mL, 50 μL) was added to each tube, contents were centrifuged, separated by solid phase extraction (Strata solid phase extraction column C18-E, 100 mg, by Phenomenex), evaporated *in vacuo* at 50 °C, and reconstituted to 50 μL prior to analysis.

Quantification of NVP and Its Metabolites from Microsomal Incubations. Samples were reconstituted to 50 μL with mobile phase (16% acetonitrile and 84% water with 2 mM ammonium acetate and 1% acetic acid). The samples were separated by HPLC and analyzed by mass spectrometry. The separation was performed on an Ultracarb C18 30 × 2.0 mm, 5 μm column (Phenomenex) under isocratic conditions with a mobile phase consisting of 16% acetonitrile and 84% water with 2 mM ammonium acetate and 1% acetic acid. The flow rate was 0.2 mL/min.

Mass Spectrometry Analysis. Mass spectrometry was carried out using a PE Sciex API 3000 quadrupole system with an electrospray ionizing source. The ion pairs used for this analysis were 267.0/226.1 for NVP, 283.1/223.1 for 12-OH-NVP, 297.1/210.1 for 4-COOH-NVP, 283.1/161.0 for 2-OH-NVP, 283.1/214.0 for 3-OH-NVP, and 255.1/227.2 for ethyl-NVP (positive ionization mode). Standard curves prepared for 2-OH-NVP (0.43−102.9 μg/mL), 3-OH-NVP (0.36−86.8 μg/mL), 12-OH-NVP (0.38−91.0 μg/mL), 4-COOH-NVP (0.26−61.8 μg/mL), and NVP (0.74−176.9 μg/mL) had R^2 values of >0.99.

Analysis of Covalent Binding Using SDS−PAGE and Immunoblotting. Livers were homogenized in working cell lysis buffer (Cell Signaling Technologies, Pickering, ON) containing 1× HALT Protease Inhibitor Cocktail (Pierce, Rockford, IL) with a Polytron 2100 homogenizer and centrifuged at 1000*g* for 15 min, and the supernatant was collected and again centrifuged at 10 000*g* for 30

min. The supernatant was mixed with Pierce reducing sample loading buffer in a 4:1 protein to buffer ratio and boiled for 5 min. Sodium dodecyl sulfate–polyacrylamide gel electrophoresis was performed using the Protean-3 minigel system (BioRad, Mississauga, ON). Gels were hand-cast (8%) or bought from Bio-Rad Canada (12%) and were run at 130 V. Electrophoresis running buffer (Bio-Rad) consisted of 25 mM Tris base, 192 mM glycine, and 0.1% sodium dodecyl sulfate, pH 8.3. Transfer to nitrocellulose membrane (0.2 μM, BioRad) occurred at 0.13 mA for 90 min at 4 °C using the same Protean-3 minigel system (BioRad, Mississauga, ON). Tris-glycine transfer buffer (Bio-Rad) consisted of 25 mM Tris, 192 mM glycine, and 20% methanol at pH 8.5. Membranes were washed twice in tris-buffered saline Tween-20 (TBST) wash solution for 5 min. Membranes were then blocked in 5% nonfat milk blocking solution in TBST. Blocking was done for 90 min at room temperature. Membranes were then rinsed with three changes of TBST for 5 min each and incubated with a 1:100 or 1:500 dilution of primary anti-NVP antiserum and 10% normal goat serum in TBST overnight at 4 °C. A 20 min wash (three changes) in TBST after overnight blocking was followed by a 90 min incubation in secondary antisera (1:2000 or 1:5000 dilution) in TBST containing 10% goat serum. The secondary antisera were goat antirabbit horseradish peroxidase antisera. Membranes were washed 3 times for 20 min with TBST. All blots were incubated with enhanced chemiluminescence stain for 5 min and analyzed with a FluorChem8800 imager. To probe for the glyceraldehyde 3-phosphate dehydrogenase (GAPDH) loading control, membranes were stripped of primary anti-NVP antiserum using Pierce Restore Plus buffer (Pierce, Rockford, IL) for 15 to 20 min at room temperature followed by a 1 h blocking step. Membranes were then incubated in mouse monoclonal anti-GAPDH antisera (1:40,000) and processed as described above except that the secondary antisera were goat antimouse horseradish peroxidase antisera diluted 1:10,000 (Jackson ImmunoResearch, Baltimore Pike, West Grove, PA.).

Analysis of *in Vivo* Covalent Binding Using Immunohistochemistry. The liver samples were fixed in 10% formalin and the paraffin block, hematoxylin/eosin slides, or unstained sections were prepared at the Toronto Hospital for Sick Children. For immunohistochemical staining, nonspecific sites were blocked with 10% goat serum for 1 h. At this point, the anti-NVP antiserum was diluted to 1:100 in 10% goat serum and applied to each section overnight. Following a washing step, slides were submerged in 0.3% hydrogen peroxide in methanol for 10 min to block endogenous peroxidases followed by a washing step. Secondary antiserum (goat antirabbit IgG-HRP conjugated antisera) was applied to the sections at a dilution of 1:3000 in 10% goat serum. Sections were incubated with secondary antiserum for 2 h. After a final washing step, Vector NovaRED stain was added as a substrate for the peroxidases following package protocol. Sections were then counterstained with Mayer's hematoxylin (Sigma), dehydrated by sequential immersion in increasing concentrations of ethanol, cleared in xylenes, and mounted using Permount mounting medium (Fisher, Markham, ON).

Plasma Alanine Transaminase and Cytokine Analysis. Alanine transaminase (ALT) was assayed using the Infinity ALT (glutamic pyruvate transaminase) Liquid Stable Reagent kit by Thermo Scientific. Screening for cytokines was performed using a Luminex immunoassay mouse cytokine/chemokine kit from Millipore Corporation (Milliplex Map Kit). Homogenized liver tissue or serum samples prepared accroding to the kit's specifications were plated and analyzed following the manufacturer's instructions.

RESULTS

Characterization of the Anti-NVP-NAC-KLH Antiserum. ELISA analysis showed that the anti-NVP-NAC-KLH antiserum recognized the NVP-NAC-BSA conjugate or KLH but not BSA alone (Figure 1A). The binding of the antisera to the NVP-NAC-BSA conjugate was inhibited by preincubating the anti-NVP-NAC-KLH antiserum with NVP or its metabolites (Figure 1B). Inhibition was much less with 2-OH-NVP, 3-OH-NVP, and 4-COOH-NVP (the metabolite in which the methyl group has been oxidized to a carboxylic acid). Binding could still be detected at an antiserum dilution of 1/1,000,000.

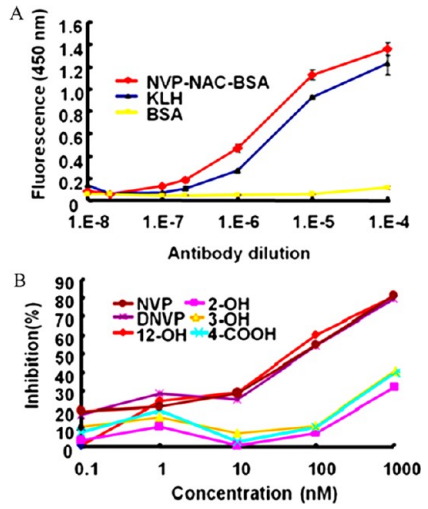

Figure 1. ELISA analysis showing (A) binding of the anti-NVP-NAC-KLH antiserum to the NVP-NAC-BSA conjugate, KLH, or BSA, and (B) the effect of preincubation of the antiserum with NVP or its metabolites on the binding of the antisera to the NVP-NAC-BSA conjugate. Data represent the mean ± SD from 3 incubations.

Covalent Binding of NVP, DNVP, or 12-OH-NVP to Hepatic Microsomes *in Vitro* and Comparison to *in Vivo* Hepatic Covalent Binding. When microsomes produced from male BN rats were incubated with NVP, 12-OH-NVP, or DNVP, the greatest covalent binding observed was with NVP, and the stongest band was at ~55 kDa (Figure 2A), which corresponds to the mass of the male dominant P450 2C11/3A1 isoforms.[14] Incubation of mouse liver microsomes with NVP produced a band of slightly higher mass, ~57 kDa (Figure 2B), corresponding to the mass of the dominant murine P450 3A11.[9] Significant covalent binding of 12-OH-NVP was not observed with rat microsomes, and DNVP produced a much fainter band at 55 kDa than NVP in both rodent species tested. *In vivo* experiments with either species displayed a wide range of covalently modified bands that were much more intense than from *in vitro* experiments. The covalent binding of DNVP to both rat and mouse hepatic microsomes was also much less than that of NVP by almost 5-fold as determined by densitometry (data not shown). The amount of binding did not increase significantly beyond 15 min (Figure 2C).

Covalent Binding of NVP to Expressed Rat CYP2C11 or CYP3A1 Supersomes, or of NVP, DNVP, or 12-OH-NVP to Human Hepatic Expressed CYP3A4 Supersomes. Incubation of NVP with expressed rat CYP2C11 (Figure 3A) or CYP3A1 Supersomes (Figure 3B), the dominant forms of P450 in male rats[14−16] led to covalent binding with major bands produced at ~50 kDa and ~52 kDa, respectively. In the absence of NVP as indicated in the figures, there is a small artifact band. Binding to 2C11 and 3A4 was strongest at 30 min; a decrease in the intensity of the P450 band was observed from 30 to 120 min.

The incubation of expressed human 3A4 displayed the greatest binding with NVP (Figure 3C) versus 12-OH-NVP or DNVP. However, 12-OH-NVP did bind to human CYP3A4 more than expected, although less than NVP, and there was much less binding of DNVP. The NVP-modified band had a mass of ~57 kDa, which is the mass of CYP3A4.[17]

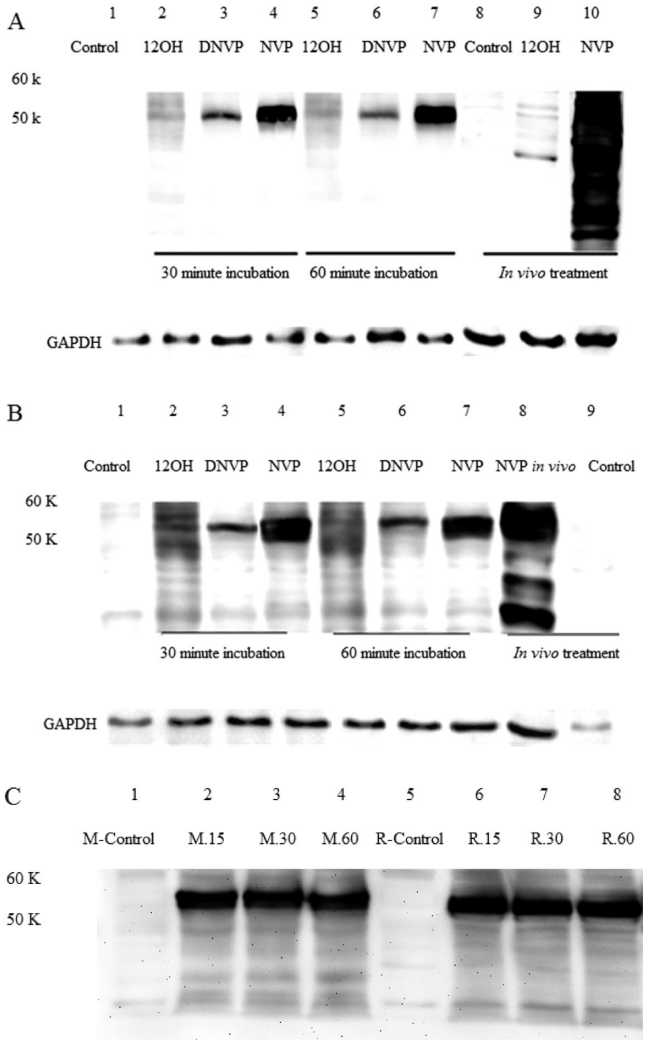

Figure 2. (A) Comparison of covalent binding of 12-OH-NVP (lanes 2 and 5) and DNVP (lane 3, 6) with that of NVP (lanes 4 and 7) after a 30 or 60 min incubation with male BN rat microsomes (1 mg/mL protein) at a drug concentration of 1 mM. For comparison, covalent binding to hepatic proteins is shown after 8 days of treatment of female rats with 12-OH-NVP (159 mg/kg/day, lane 9) or NVP (150 mg/kg/day, lane 10). Protein loading was 15 μg for lanes 1−7 and 20 μg for lanes 8−10. (B) Comparison of covalent binding of 12-OH-NVP (lanes 2, 5) and DNVP (lanes 3 and 6) with that of NVP (lanes 4 and 7) at a concentration of 1 mM after a 30 or 60 min incubation with microsomes (1 mg/mL protein) from male C57BL/6 mice. For comparison, covalent binding to hepatic proteins is shown after 6 weeks of treatment of C57BL/6 mice with NVP at a dose of 950 mg/kg/day in food. Protein loading was 13 μg for lanes 1−7 and 20 μg for lanes 8−9. (C) Comparison of covalent binding of NVP to hepatic microsomes from male C57BL/6 mice (lanes 2−4) or male BN rats (lanes 6−8) after a 15, 30, or 60 min incubation at a drug concentration of 1 mM and microsome concentration of 1 mg/mL protein. Protein loading was 20 μg per lane. The primary antiserum dilution was 1:500, and that of the secondary antisera was 1:5000.

Covalent binding of NVP or 12-OH-NVP to Hepatic Proteins from Female BN Rats Treated with NVP or 12-OH-NVP. Female BN rats were treated with NVP or 12-OH-NVP for a period of 8 days at doses of 150 mg/kg/day or 159 mg/kg/day, respectively (Figure 4). The pattern of covalent binding was different for NVP and 12-OH-NVP; this difference was most prominent for the lower molecular mass proteins

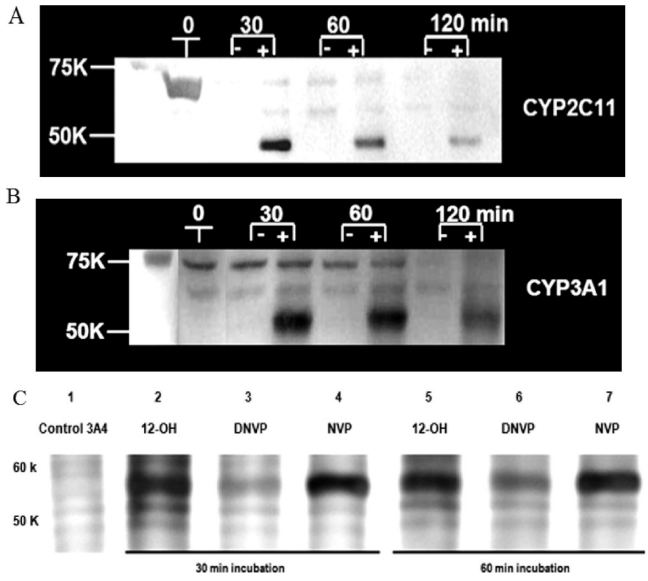

Figure 3. Covalent binding of NVP to expressed male rat CYP2C11 (A) or CYP3A1 (B) *in vitro*. Protein concentration for each incubation was 0.8 mg/mL with 0.5 mM of drug. For immunoblots, protein loading was 9 μg and 7.5 μg per lane for A and B, respectively. (+) indicates incubations containing NVP, while (−) indicates incubations lacking NVP. Proteins were resolved on 12% gels with 1:100 dilution of primary antiserum followed by 1:2000 dilution of secondary antisera. Comparison of covalent binding of 12-OH-NVP (lanes 2 and 5) or DNVP (lanes 3 and 6) with that of NVP (lanes 4 and 7) to human CYP3A4 with a drug concentration of 1 mM and protein concentration in each incubation of 1 mg/mL (C). Proteins (10 μg/lane) were resolved on an 8% gel. Dilutions of antisera were 1:500 for the primary antiserum and 1:5000 for the secondary antiserum.

(30− 60 kDa). NVP-treated female BN rats exhibited greater covalent binding than 12-OH-NVP-treated rats at an equimolar dose, but there was a prominent artifact band in the 12-OH-NVP blot at about 60 kDa. Preincubation of the anti-NVP serum with NVP blocked almost all of the binding (Figure 4B).

Immunohistochemistry of Liver from NVP- or DNVP-Treated or NVP + ABT Co-treated Female BN Rats. Hepatic covalent binding of NVP and DNVP was greatest in the centrilobular area (Figure 5). The pattern of binding was dramatically different in rats treated with a combination of NVP and the P450 inhibitor aminobenzotriazole; specifically, treatment with ABT blocked binding in the centrilobular area and shifted it to the periportal area. Co-treatment with ABT also changed the pattern of binding by Western blot, although there was still significant binding (data not shown). Clearance of NVP depends on oxidative metabolism, and so even if P450 is inhibited, it causes an increase in blood levels, but ultimately NVP is oxidized.

Oxidation of NVP or 12-OH-NVP by Rat Liver Microsomes. The carboxylic acid (4-COOH-NVP) of NVP was detected in the incubation of 12-OH-NVP with NADPH and hepatic microsomes from both male and female BN rats (Figure 6). No aldehyde intermediate was detected in these reactions.

Covalent Binding, Serum ALT levels, INF-γ, and IL-6 Levels in Mice. There was no change in plasma ALT in BN rats treated with NVP (data not shown). Various strains of mice were treated with NVP to determine if it causes liver damage, covalent binding, and/or histological changes. Male BALB/c mice treated with NVP had no increase in ALT (data not

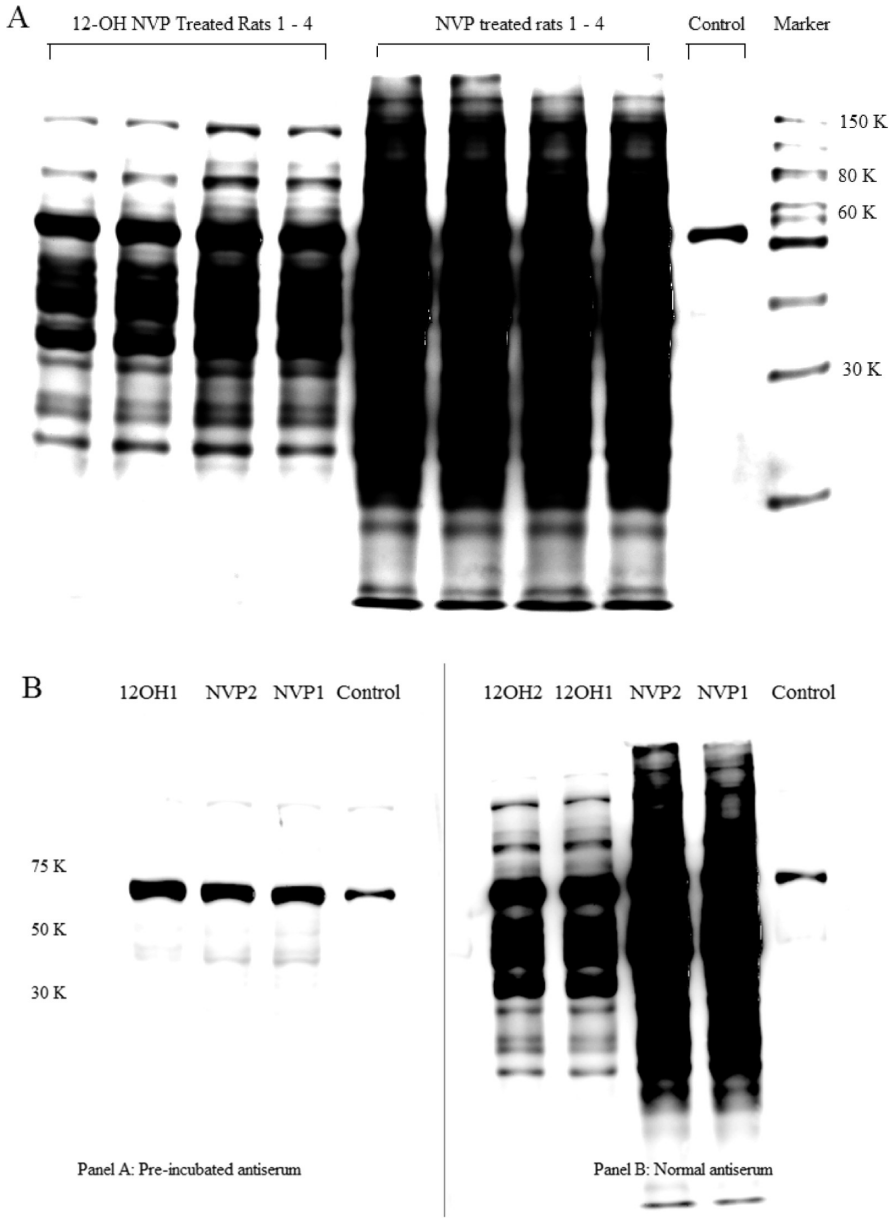

Figure 4. (A) Covalent binding to hepatic proteins from female BN rats fed NVP (150 mg/kg) or 12-OH-NVP (159 mg/kg) for 8 days. Protein loading was 12 μg per lane. Samples were resolved on an 8% gel. A 1:500 dilution of primary antiserum was followed by 1:5000 dilution of secondary antisera. (B) Incubation of the anti-NVP serum with 2 mM NVP for 2 h at 37 °C blocked most of the binding (left side of panel) to samples from livers of 12-OH or NVP treated rats. Samples for both panels A and B were prepared, run, blocked, incubated with secondary antibody, and imaged at the same time, and protein loading was 10 μg/well of protein per lane.

shown), while there was an increase in ALT in male C57BL/6 mice at 3 weeks followed by normalization of ALT levels (Figure 7A). Immunoblots revealed no significant differences between the pattern and degree of binding in these two strains (Figure 7B). ALT levels in both male and female Cbl-b$^{-/-}$ mice increased at week 2, with a somewhat greater increase in male mice (Figure 8A) than female mice (Figure 8C). The animals with the largest ALT increase displayed areas of gross hepatic necrosis evident as areas of white on the surface of the liver upon sacrifice at 2 weeks. Immunoblot analysis showed the presence of a wide range of modified hepatic protein in both male (Figure 8B) and female (Figure 8D) mice. Animals with gross necrosis appeared to have slightly more binding of NVP to lower molecular mass proteins (Figure 8B,D).

Luminex analysis for a broad range of cytokines performed on serum of mice from the 2 week study on days 1, 7, and 14 of NVP treatment revealed an increase in interferon-gamma (IFN-γ) in plasma samples of male mice on day 7 (Figure 9B), both in animals that developed significant necrosis and those that did not, but the level was highest in an animal that did develop necrosis. IL-6 was also increased at day 7 versus day 14 of NVP treatment in plasma of male mice (Figure 9A). By day 14 of NVP treatment, the cytokine levels had decreased to or close to the baseline (data not shown) for the majority of animals.

Changes in cytokines were less clear for serum samples from female Cbl-b $^{-/-}$ mice, and no inferences could be made (data not shown). No significant changes in cytokines were observed for GM-CSF, IL-10, 1 L-12(p70), IL-13, IL-17, 1 L-1β, IL-2, IL-4, IL-5, IL-7, IL-9, MCP-1, or TNF-α.

dx.doi.org/10.1021/tx300172s | *Chem. Res. Toxicol.* 2012, 25, 1708−1719

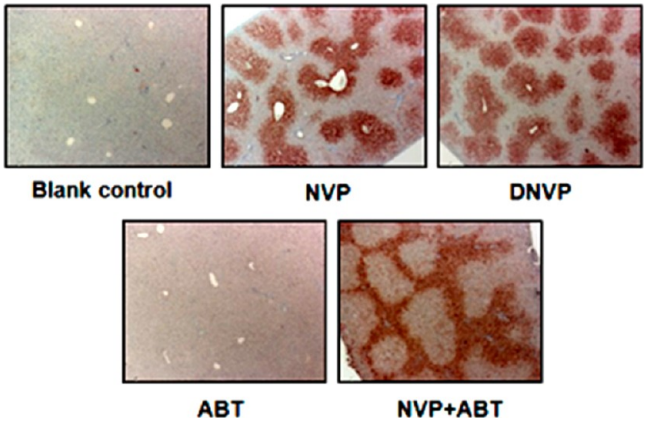

Figure 5. Immunohistochemistry of liver sections from female BN rats; blank control, NVP treatment (150 mg/kg/day × 7 days in food), DNVP treatment (150 mg/kg/day × 7 days in food), ABT treatment (50 mg/kg/day × 28 days by gavage), or NVP (150 mg/kg/day) + ABT (50 mg/kg/day) × 28 days by gavage. Slides were incubated with 1:100 dilution of primary antisera and 1:2000 dilution of the secondary antisera. The slides were counterstained with Mayer's hematoxylin; magnification 20×.

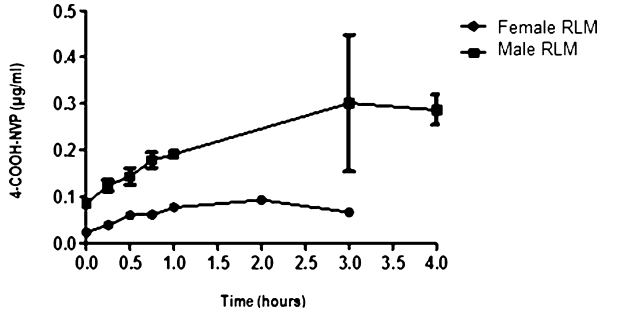

Figure 6. 4-COOH-NVP concentrations from incubations of 12-OH-NVP with microsomes from male (n = 3) and female (n = 1) BN rats.

Liver Histology and ALT in Male Cbl-b$^{-/-}$ or C57BL/6 Mice Treated with NVP. Liver histology of Cbl-b$^{-/-}$ mice sacrificed after 2 weeks of NVP treatment at the time of maximal ALT elevation is shown in Figure 10. The presence of gross necrosis, which was visible on the surface of the liver as white areas was observed in 4 of 7 treated animals. Three NVP-treated males with gross liver necrosis had ALT values ≥200 U/L. Two of 8 NVP-treated female mice with minor liver necrosis had ALT values of 286 and 80 U/L. Histology in female mice did not demonstrate as much injury as in males (data not shown). Histology of the livers of affected males showed the presence of focal subcapsular areas of massive liver necrosis (Figure 10B,C) sharply demarcated from the adjacent viable liver. Necrotic areas were surrounded by and infiltrated by mononuclear cells, macrophages, and neutrophils. This pattern of liver necrosis suggests an ischemic injury, but no evidence of thrombi or vasculitis was observed. Multifocal necro-inflammatory hepatitis with neutrophil-rich inflammatory response was observed in the absence gross necrotic lesions in male Cbl-b$^{-/-}$ mouse livers. Lower doses of NVP were also tested with Cbl-b$^{-/-}$ mice, but no injury was seen (data not shown). In contrast, hepatic histology of C57BL/6 mice treated with NVP and sacrificed at 4 weeks displayed hepatocyte death on the edge of the lobe in one animal, as well as small focal areas of necrosis (Figure 11B). Induction of smooth endoplasmic reticulum (Figure 11C), presumably including P450 induction, was present in the histology of all mice strains tested but was most prominent for Cbl-b$^{-/-}$ male mice. This marked induction may have led to greater reactive metabolite formation contributing to the greater toxicity in this strain, and this appeared to be the case although the difference is subtle (Figure 12).

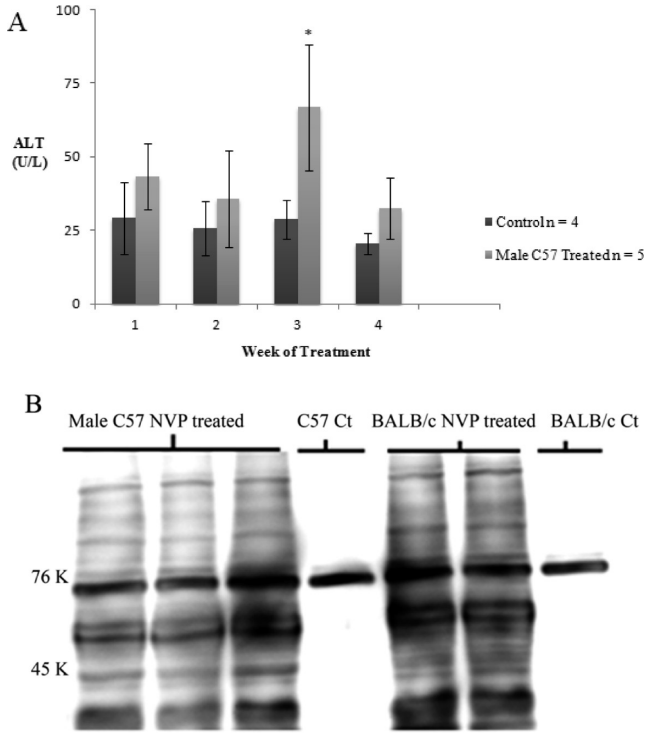

Figure 7. (A) Changes in ALT in male C57BL/6 mice treated with NVP (950 mg/kg/day) for 4 weeks. Values are based on the mean of triplicate readings per time point per animal ± SD, n = 5 treated mice or n = 4 control mice. Unpaired t test, 7 d.f., p < 0.05. (B) Corresponding covalent binding of NVP at the same dose in male BALB/c (n = 2) or C57BL/6 (n = 3) mouse livers after 6 weeks of treatment. Protein loading was 20 µg per lane. Samples were resolved on an 8% gel.

Comparison of Hepatic Covalent Binding of NVP between Mice and Female BN Rats. Female BN rats treated with NVP for 1, 2, 4, or 8 days were sacrificed, and covalent binding was determined (Figure 12). In comparison with Cbl-b$^{-/-}$ knockout mice at 2 or 10 weeks of treatment or male C57BL/6 mice at 2 weeks of treatment, rats had significantly greater binding from day 4 onward. In all animals, the presence of a modified P450 band at ~55 kDa was prominent and represents the largest modified band in each lane. While modified proteins in rats range from 20 to 100 kDa, it appeared that lower molecular weight proteins were modified in mice (up to 70 kDa). Treatment of Cbl-b$^{-/-}$ mice with NVP for 2 weeks led to greater binding than that at 10 weeks, and C57BL/6 mice displayed the least binding of the species tested.

DISCUSSION

An anti-NVP antiserum was produced and used to demonstrate that NVP covalently binds to hepatic proteins, both in *vitro* and *in vivo*. Binding occurred directly to P450 as demonstrated by covalent binding to expressed P450s, both rat and human. We have shown that the skin rash requires oxidation of NVP to 12-OH-NVP,[6] and most recently, we have shown that covalent

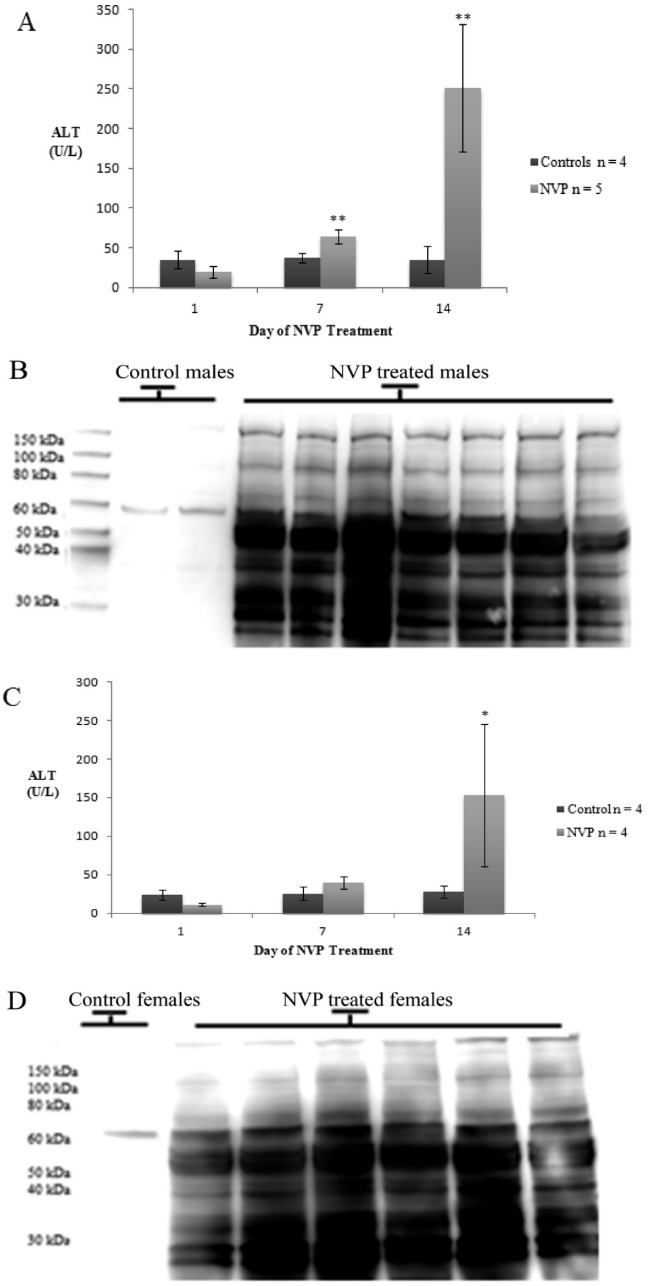

Figure 8. (A) Plasma ALT levels in male Cbl-b$^{-/-}$ mice fed NVP orally for 14 days (950 mg/kg/day). Values are based on the mean of triplicate readings per time point per animal ± SD, n = 5 treated mice or n = 4 control mice. Unpaired t test, 7 d.f., $p < 0.05$. (B) Covalent binding of NVP in the livers of the same Cbl-b$^{-/-}$ mice. (C) Plasma ALT levels in NVP-treated (950 mg/kg/day) female Cbl-b$^{-/-}$ mice, n = 4 treated or n = 4 control mice. Values are based on the mean of triplicate readings per time point per animal ± SD, n = 5 treated mice or n = 4 control mice. Unpaired t test, 6 d.f., $p < 0.05$. (D) Covalent binding of NVP in the livers of the same mice. Protein loading was 25 μg per lane. Samples were resolved on 10−20% gradient gels. A 1:500 dilution of primary antisera followed by 1:5000 dilution of secondary antisera was used.

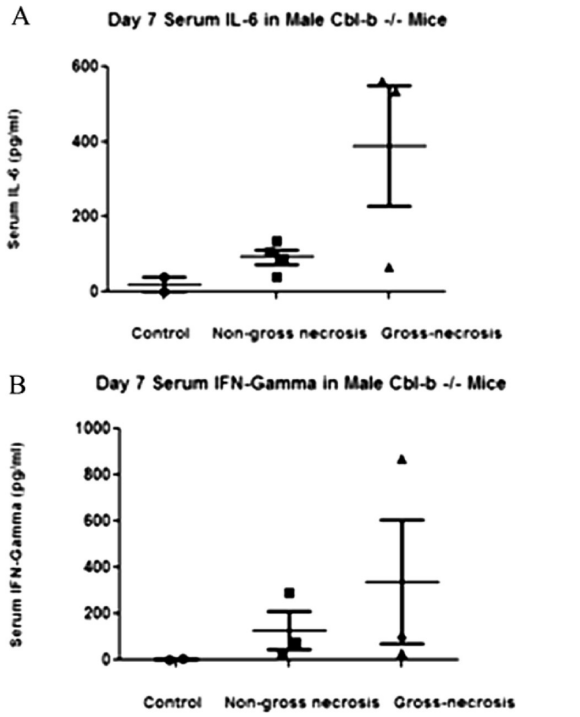

Figure 9. Serum IL-6 (A) or IFN-γ (B) from control and NVP-treated Cbl-b$^{-/-}$ mice at day 7 of NVP treatment. Animals showing gross necrosis are displayed separately.

binding of the benzylic sulfate of this metabolite formed by sulfotransferase in the skin is responsible for the rash (manuscript in preparation). In contrast, the majority of binding in the liver must involve direct oxidation by P450 as evidenced by the marked shift in the pattern of binding from the centrilobular region to the portal region caused by the P450 inhibitor ABT, as shown in Figure 5. There is also less covalent binding of 12-OH-NVP than NVP in the liver. Furthermore, substitution of the methyl hydrogens with deuterium (DNVP) led to a marked decrease in covalent binding. Given that oxidation of the methyl group is involved in the covalent binding, but it does not involve 12-OH-NVP, these data provide strong evidence that the chemical species responsible for the covalent binding in the liver is a quinone methide formed by the loss of a hydrogen atom from the P450-generated free radical (TOC graphic). Others have found evidence for an epoxide reactive metabolite,[8] but these data suggest that it is less important with respect to covalent binding than the quinone methide.

Some covalent binding of 12-OH-NVP was detected in the *in vitro* experiments where phase II pathways such as sulfation would not occur, and the pattern of binding was somewhat different from that of NVP. This suggests that oxidation of 12-OH-NVP can lead to a reactive metabolite, although the binding is less than that for NVP. This could be due to oxidation of the benzylic alcohol to an aldehyde or oxidation of some other part of the molecule. Oxidation of 12-OH-NVP by rat hepatic microsomes led to the carboxylic acid (TOC graphic), but the intermediate aldehyde was not observed (Figure 6). This suggests that 12-OH-NVP is oxidized all the way to the carboxylic acid by P450 without release of the intermediate aldehyde; there is precedent for this.[6] It is conceivable that some of the aldehyde could become covalently bound to P450 and be responsible for the observed covalent binding; however, the pattern of binding was broader than that of NVP; specifically, most of the binding was to proteins with masses different from P450. Therefore, the aldehyde seems unlikely to be responsible for a significant amount of the covalent binding of 12-OH-NVP. To re-emphasize, the data

dx.doi.org/10.1021/tx300172s | *Chem. Res. Toxicol.* 2012, 25, 1708−1719

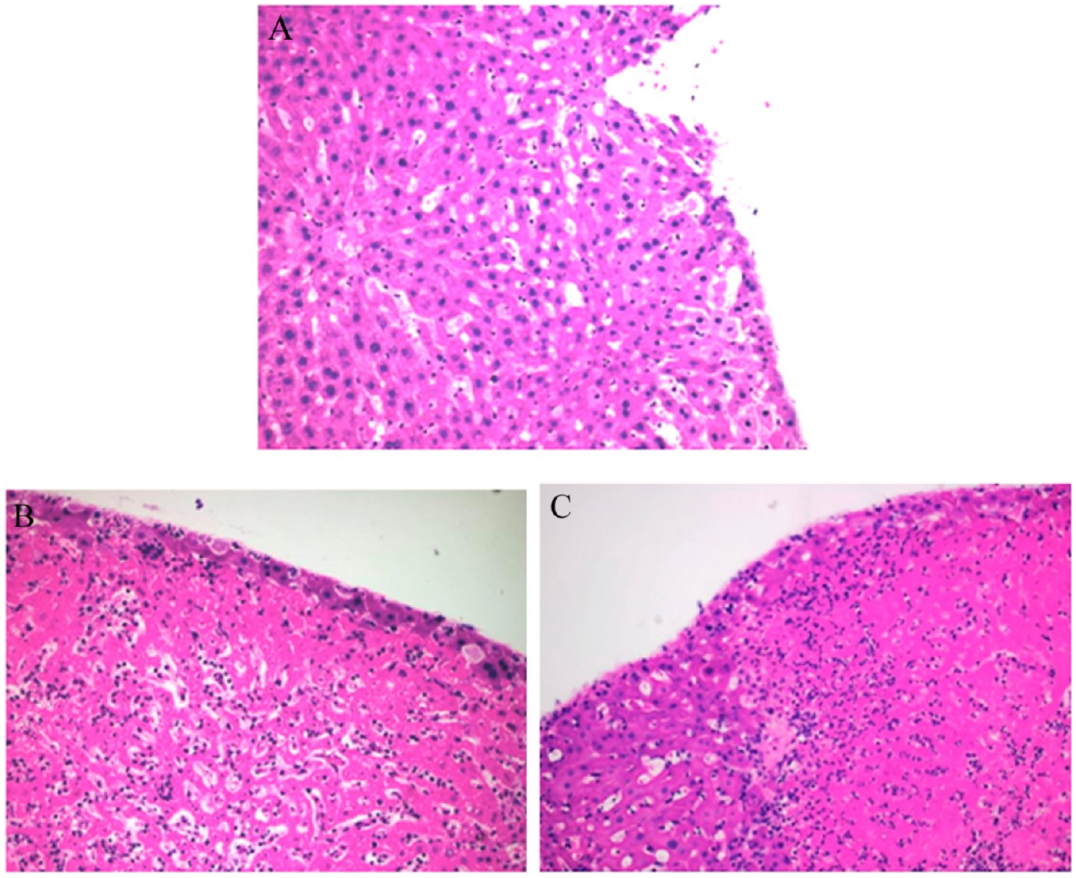

Figure 10. H&E staining of livers from Cbl-b$^{-/-}$ mice treated with NVP for 2 weeks. (A) Untreated control liver with normal ALT; (B) the liver from a NVP-treated mouse with gross necrosis and an ALT of 271 U/L, and the (C) liver from another NVP-treated mouse with gross necrosis and ALT of 313 U/L. Areas of massive hepatocyte necrosis surrounded by viable hepatocytes are shown in B and C.

strongly implicate the quinone methide as being the major species responsible for covalent binding of NVP in the liver.

Although we had previously observed some strange inclusion bodies in the livers of rats treated with NVP, we did not observe an increase in ALT even though there was a significant degree of covalent binding. This suggests that covalent binding may be necessary but not sufficient to produce liver injury; this is consistent with an immune mechanism. We attempted to develop an animal model of NVP-induced liver toxicity in mice. Mice metabolize NVP much faster than rats, and even higher doses did not produce easily detectable blood levels of NVP or outward signs of toxicity. However, even with higher doses and more rapid metabolism, the amount of covalent binding in mice was less than that in BN rats. Treatment of C57BL/6 mice with NVP led to a small increase in ALT in some animals that resolved despite continued treatment. This is the pattern of adaptation frequently observed in humans treated with a drug that can cause more severe idiosyncratic liver injury. Liver histology in these mice revealed moderate inflammatory nodules and areas of mild focal necrosis (Figure 11B,C). Although the covalent binding in BALB/c mice was similar to that in C57BL/6 mice, no increase in ALT was observed in BALB/c mice. We then treated Cbl-b knockout mice with NVP. Cbl-b$^{-/-}$ mice lack E3 ubiquitin ligase, which leads to impaired immune tolerance; however, the animals are phenotypically normal. This deficiency could also lead to increased covalent binding if ubiquitin ligase is required for clearance of modified proteins, and this appeared to be the case (Figure 12). We found that there was a much greater increase in ALT in some of the Cbl-b$^{-/-}$ mice than in the C57BL/6 mice, but the ALT also returned to normal despite continued treatment with the drug. Histology performed at the time of peak ALT (14 days) showed areas of complete necrosis with a local inflammatory response. These appeared to represent ischemic lesions because cells close to the liver capsule were spared presumably because they could benefit from diffusion through the liver capsule. However, no vascular lesions were evident histologically.

Luminex analysis of cytokines performed on serum samples from Cbl-b$^{-/-}$ mice sacrificed at the time of ALT peak displayed a significant increase in serum IFN-γ and IL-6 in some of the animals (Figure 9A,B). This increase was most prominent on day 7 rather than day 1 or 14 in the majority of mice, and it occurred before the ALT increase at day 14. An elevation in cytokines or immune factors that occurs earlier than increases in other toxicity markers (i.e., ALT) is consistent with an immune response. At the study end point of 14 days, IFN-γ in liver samples of male Cbl-b$^{-/-}$ mice was also elevated to ~100 pg/mL for two mice (data not shown) with gross necrosis compared with 39 pg/mL for control mice. One mouse with elevated IFN-γ in the liver (130 pg/mL) on day 14 also had markedly elevated plasma IFN-γ (866 pg/mL) on day 7 of treatment. This cytokine is considered a pro-hepatotoxic mediator leading to inflammation and tissue injury through activation of macrophages and natural killer cells.[18] This is consistent with a clinical study performed by Keane et al. that found that incubation of NVP with T-cells from a patient with

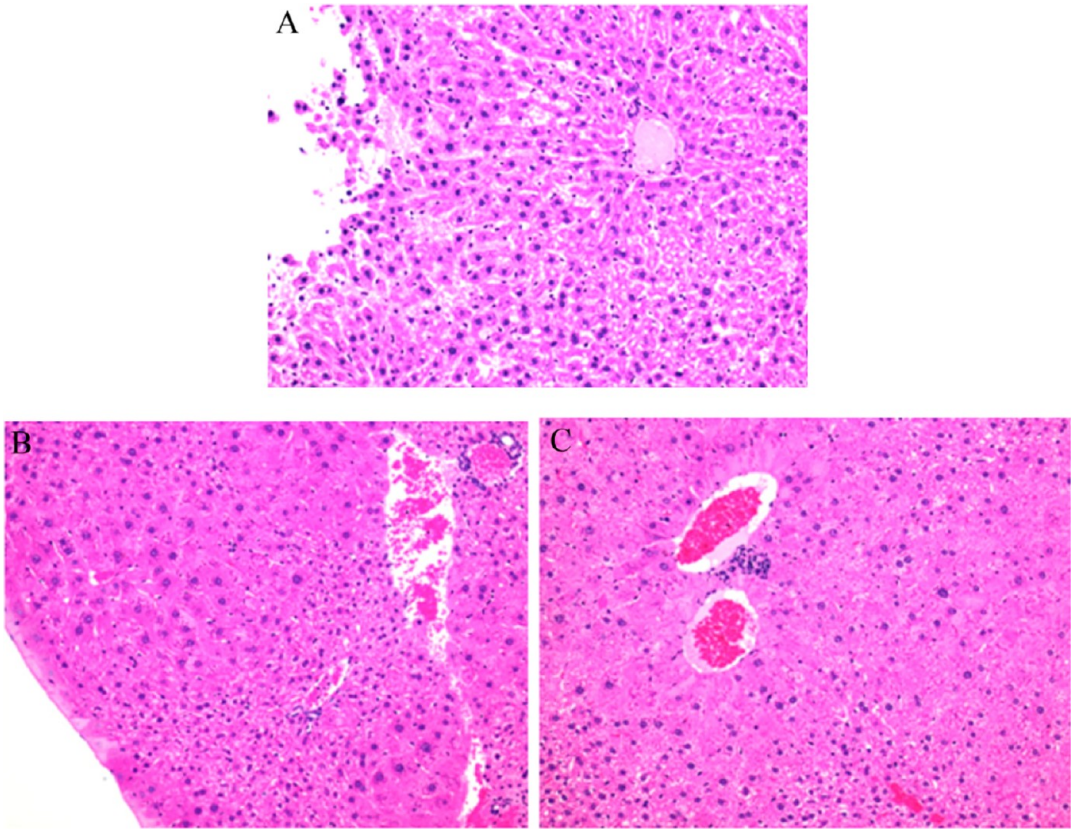

Figure 11. H&E staining of livers from male C57BL/6 mice treated with NVP for 3 weeks. (A) Untreated control liver with a normal ALT; (B) the liver from a NVP-treated mouse with very mild necrosis (appearing as the thin band around the capsule) and ALT of 94 U/L; and (C) the liver from another NVP-treated mouse with an ALT of 75 U/L. Changes to the liver parenchyma due to enlargement of hepatocytes in the periacinar regions and extensive expansion of the endoplasmic reticulum are also present in both B and C.

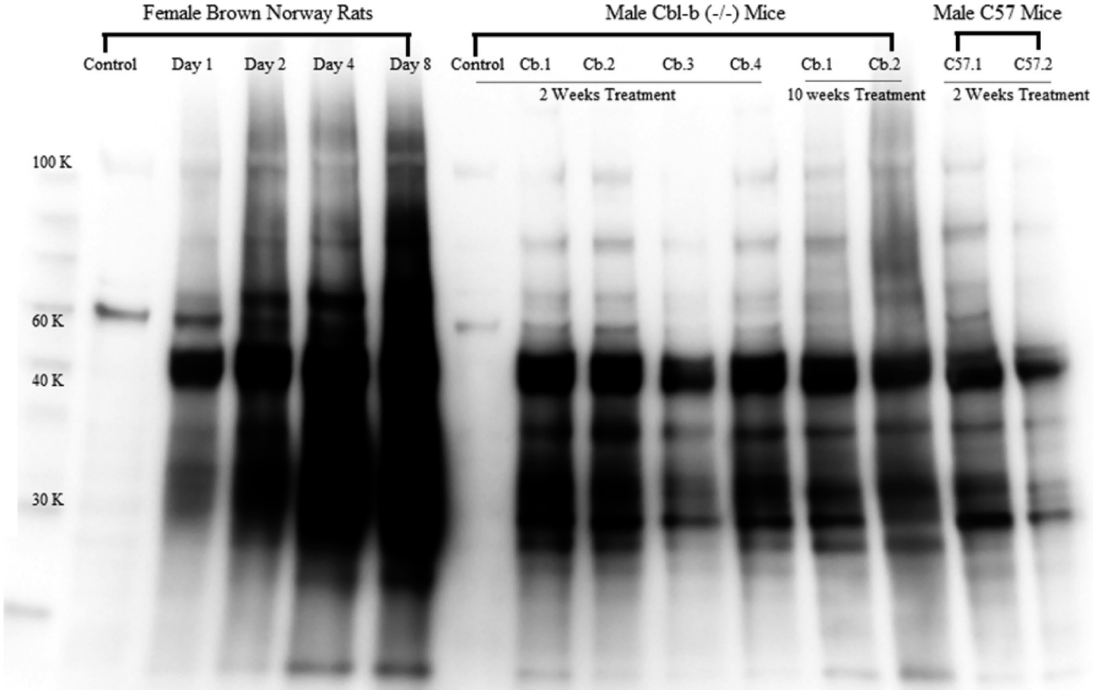

Figure 12. Comparison of covalent binding of NVP to hepatic proteins in mice and rats. NVP was fed to rats in a time course manner from 1 to 8 days at 150 mg/kg orally in food. Mice were given 950 mg/kg/day for 2 weeks or 10 weeks. C57BL/6 males given NVP for 2 weeks are represented by C57.1 and C57.2. Each lane was loaded with 20 μg of protein. Samples were resolved on a 4−20% gradient gel. A 1:500 dilution of primary antisera followed by a 1:5000 dilution of secondary antisera was used.

dx.doi.org/10.1021/tx300172s | *Chem. Res. Toxicol.* 2012, 25, 1708−1719

NVP-induced skin rash led to the production of IFN-γ by T cells.[19]

Reviews regarding the difficulties with production of animal models of idiosyncratic drug reactions are available elsewhere, but the major obstacle appears to be the development of immune tolerance.[20] This is consistent with the delayed onset of liver injury and resolution despite continued treatment observed in these mice. We suspect that the liver injury in humans is immune-mediated and that the reason that most humans and rats do not develop liver injury is that the dominant response is immune tolerance. It is known that the dominant immune response in the liver is tolerance[18] and that it is presumably why liver transplantations are relatively easy compared to transplantation of, for example, skin. Co-treatment of Cbl-b$^{-/-}$ mice with polyinosinic/polycytidylic acid, imiquimod, and even γ-irradiation to deplete circulating regulatory T-cells was used in an attempt to break the immune tolerance and induce sustained liver damage. All of these attempts were unsuccessful in both male and female mice (data not shown).

A clear picture regarding the specific types of proteins covalently modified by hepatotoxic drugs and the outcome of liver injury does not exist. Therefore, even though mice and rats display a relatively similar pattern of NVP-induced covalent binding, other individual or species-specific factors must play a role in the development of liver injury. In support of this, a recent clinical study demonstrated that patients who carried the HLA-DRB*01 allele were at increased risk of developing NVP-induced liver toxicity (the alleles associated with the risk of skin rash were different), but there was no association with the CYP2B6 genotype, which is polymorphic and is one of the P450s involved in the metabolism of NVP.[21,22]

In conclusion, we have clearly demonstrated that NVP covalently binds to hepatic proteins in mice, rats, and humans. The major chemical species responsible for this covalent binding is a quinone methide metabolite. We have shown a mild delayed-onset liver injury in C57BL/6 mice that may be the basis for an animal model if a method can be found to increase liver injury. More significant injury was observed in Cbl-b$^{-/-}$ mice, but the histology suggests that the mechanism may be different.

AUTHOR INFORMATION

Corresponding Author

*Leslie Dan Faculty of Pharmacy, University of Toronto, 144 College St., Toronto ON, M5S 3M2, Canada. Phone: 416-978-8939. Fax: 416-978-8511. E-mail: jack.uetrecht@utoronto.ca.

Funding

A.S. is the recipient of a University of Toronto Pharmaceutical Sciences Fellowship. J.U. is the recipient of the Canada Research Chair in Adverse Drug Reactions. This work was supported by a grant received from the Canadian Institutes of Health Research (MOP84520).

Notes

The authors declare no competing financial interest.

ACKNOWLEDGMENTS

We thank Boehringer-Ingelheim for supplying nevirapine. Portions of this work were parts of presentations given by A. M. Sharma and J. P. Uetrecht at the Society of Toxicology International Meetings in Salt Lake City, UT, in 2010, and Washington, D.C., in 2011.

ABBREVIATIONS

ABT, 1-aminobenzotriazole; BN, Brown Norway; BSA, bovine serum albumin; 12-OH-NVP, 12-hydroxynevirapine; DNVP, 12-trideutero-nevirapine; P450, cytochrome P450; DILI, drug-induced liver injury; GSH, glutathione; GAPDH, glyceraldehyde 3-phosphate dehydrogenase; HIV, human immunodeficiency virus; IDR, idiosyncratic drug reaction; IFN-γ, interferon-gamma; LC/MS, liquid chromatography/mass spectrometry; NVP, nevirapine; TBST, tris-buffered saline Tween-20

REFERENCES

(1) Shenton, J. M., Popovic, M., Chen, J., Masson, M. J., and Uetrecht, J. P. (2005) Evidence of an immune-mediated mechanism for an idiosyncratic nevirapine-induced reaction in the female Brown Norway rat. *Chem. Res. Toxicol. 18*, 1799−1813.

(2) Pollard, R. B., Robinson, P., and Dransfield, K. (1998) Safety profile of nevirapine, a nonnucleoside reverse transcriptase inhibitor for the treatment of human immunodeficiency virus infection. *Clin. Ther. 20*, 1071−1092.

(3) MacGregor, T. R., and Hall, D. B. (2007) Case-control exploration of relationships between early rash or liver toxicity and plasma concentrations of nevirapine and primary metabolites. *HIV Clin. Trials 8*, 391−399.

(4) Patel, S. M., Johnson, S., Belknap, S. M., Chan, J., Sha, B. E., and Bennett, C. (2004) Serious Adverse Cutaneous and Hepatic Toxicities Associated With Nevirapine Use by Non-HIV-Infected Individuals. *JAIDS 35*, 120−125.

(5) Shenton, J. M., Teranishi, M., Abu-Asab, M. S., Yager, J. A., and Uetrecht, J. P. (2003) Characterization of a potential animal model of an idiosyncratic drug reaction: nevirapine-induced skin rash in the rat. *Chem. Res. Toxicol. 16*, 1078−1089.

(6) Chen, J., Mannargudi, B. M., Xu, L., and Uetrecht, J. (2008) Demonstration of the metabolic pathway responsible for nevirapine-induced skin rash. *Chem. Res. Toxicol. 21*, 1862−1870.

(7) Wen, B., Chen, Y., and Fitch, W. L. (2009) Metabolic activation of nevirapine in human liver microsomes: dehydrogenation and inactivation of cytochrome P450 3A4. *Drug Metab. Dispos. 37*, 1557−1562.

(8) Srivastava, A., Lian, L.-Y., Maggs, J. L., Chaponda, M., Pirmohamed, M., Williams, D. P., and Park, B. K. (2010) Quantifying the metabolic activation of nevirapine in patients by integrated applications of NMR and mass spectrometries. *Drug Metab. Dispos. 38*, 122−132.

(9) Zimmermann, C., van Waterschoot, R. A. B., Harmsen, S., Maier, A., Gutmann, H., and Schinkel, A. H. (2009) PXR-mediated induction of human CYP3A4 and mouse Cyp3a11 by the glucocorticoid budesonide. *Eur. J. Pharm. Sci. 36*, 565−571.

(10) Grozinger, K. G., Fuchs, V., Hargrave, K. D., Mauldin, S., Vitous, J., Campbell, S., and Adams, J. (1995) Synthesis of nevirapine and its major metabolite. *J. Heterocycl. Chem. 32*, 259−263.

(11) Kelly, T. A., Proudfoot, J. R., McNeil, D. W., Patel, U. R., David, E., Hargrave, K. D., Grob, P. M., Cardozo, M., Agarwal, A., and Adams, J. (1995) Novel non-nucleoside inhibitors of human immunodeficiency virus type 1 reverse transcriptase. 5. 4-Substituted and 2,4-disubstituted analogs of nevirapine. *J. Med. Chem. 38*, 4839−4847.

(12) Chauret, N., Gauthier, A., and Nicoll-Griffith, D. A. (1998) Effect of common organic solvents on in vitro cytochrome P450-mediated metabolic activities in human liver microsomes. *Drug Metab. Dispos. 26*, 1−4.

(13) Reid, M. J., Lamé, M. W., Morin, D., Wilson, D. W., and Segall, H. J. (1998) Involvement of cytochrome P450 3A in the metabolism and covalent binding of 14C-monocrotaline in rat liver microsomes. *J. Biochem. Mol. Toxic. 12*, 157−166.

(14) Omiecinski, C. J., Hassett, C., and Costa, P. (1990) Developmental expression and in situ localization of the phenobarbi-

tal-inducible rat hepatic mRNAs for cytochromes CYP2B1, CYP2B2, CYP2C6, and CYP3A1. *Mol. Pharmacol. 38*, 462−470.
(15) Pampori, N. A., and Shapiro, B. H. (1994) Over-expression of CYP2C11, the major male-specific form of hepatic cytochrome P450, in the presence of nominal pulses of circulating growth hormone in adult male rats neonatally exposed to low levels of monosodium glutamate. *J. Pharmacol. Exp. Ther. 271*, 1067−1073.
(16) Kato, R., and Yamazoe, Y. (1992) Sex-specific cytochrome P450 as a cause of sex-and species-related differences in drug toxicity. *Toxicol. Lett. 64−65*, 661−667.
(17) Yano, J. K., Wester, M. R., Schoch, G. A., Griffin, K. J., Stout, C. D., and Johnson, E. F. (2004) The structure of human microsomal cytochrome P450 3A4 determined by X-ray crystallography to 2.05-A resolution. *J. Biol. Chem. 279*, 38091−38094.
(18) Holt, M. P., and Ju, C. (2006) Mechanisms of drug-induced liver injury. *AAPS J. 8*, E48−54.
(19) Keane, N., et al. (2007) *Proceedings of the 4th International AIDS Society Conference on HIV Pathogenesis, Treatment and Prevention*, Sydney, Australia.
(20) Shenton, J. M., Chen, J., and Uetrecht, J. P. (2004) Animal models of idiosyncratic drug reactions. *Chem-Biol. Interact. 150*, 53−70.
(21) Yuan, J., Guo, S., Hall, D., Cammett, A. M., Jayadev, S., Distel, M., Storfer, S., Huang, Z., Mootsikapun, P., Ruxrungtham, K., Podzamczer, D., and Haas, D. W. (2011) Toxicogenomics of nevirapine-associated cutaneous and hepatic adverse events among populations of African, Asian, and European descent. *AIDS 25*, 1271−1280.
(22) Mallal, S., Nolan, D., Witt, C., Masel, G., Martin, A. M., Moore, C., Sayer, D., Castley, A., Mamotte, C., Maxwell, D., James, I., and Christiansen, F. T. (2002) Association between presence of HLA-B*5701, HLA-DR7, and HLA-DQ3 and hypersensitivity to HIV-1 reverse-transcriptase inhibitor abacavir. *Lancet 359*, 727−732.